

Planar and Toroidal Morphs Made Easier

Jeff Erickson¹  Patrick Lin¹ 

¹Department of Computer Science,
University of Illinois Urbana-Champaign

| | | |
|-----------------------------|-----------------------------------------|--------------------------|
| Submitted: November 2021 | Reviewed: March 2022 | Revised: June 2022 |
| Accepted: October 2022 | Final: October 2022 | Published: February 2023 |
| Article type: Regular paper | Communicated by: I. Rutter, H. Purchase | |

Abstract. We present simpler algorithms for two closely related morphing problems, both based on the barycentric interpolation paradigm introduced by Floater and Gotsman, which is in turn based on Floater’s asymmetric extension of Tutte’s classical spring-embedding theorem.

First, we give a very simple algorithm to construct piecewise-linear morphs between planar straight-line graphs. Our algorithm entirely avoids the classical edge-collapsing strategy dating back to Cairns; instead, in each morphing step, we interpolate the pair of weights associated with a single edge. Specifically, given equivalent straight-line drawings Γ_0 and Γ_1 of the same 3-connected planar graph G , with the same convex outer face, we construct a morph from Γ_0 to Γ_1 that consists of $O(n)$ unidirectional morphing steps, in $O(n^{1+\omega/2})$ time, where n is the number of vertices and ω is the matrix multiplication constant.

Second, we describe a natural extension of barycentric interpolation to geodesic graphs on the flat torus. Barycentric interpolation cannot be applied directly in this setting, because the linear systems defining intermediate vertex positions are not necessarily solvable. We describe a simple scaling strategy that circumvents this issue. Computing the appropriate scaling requires $O(n^{\omega/2})$ time, after which we can compute the drawing at any point in the morph in $O(n^{\omega/2})$ time. Our algorithm is considerably simpler than the recent algorithm of Chambers, Erickson, Lin, and Parsa, and produces more natural morphs. Our techniques also yield a simple proof of a conjecture of Connelly, Henderson, Ho, and Starbird for geodesic torus triangulations.

Special Issue on the 29th Int. Symposium on Graph Drawing and Network Visualization, GD 2021

A preliminary version of this paper appeared in [26]

E-mail addresses: jeffe@illinois.edu (Jeff Erickson) plin25@illinois.edu (Patrick Lin)



This work is licensed under the terms of the [CC-BY](https://creativecommons.org/licenses/by/4.0/) license.

1 Introduction

Computing morphs between geometric objects is a fundamental problem that has been well studied, with many applications in graphics, animation, modeling, and more. A particularly well-studied setting is that of morphing between planar straight-line graphs. Formally, a morph between two equivalent planar straight-line graphs Γ_0 and Γ_1 consists of a continuous family of planar straight-line graphs Γ_t starting at Γ_0 and ending at Γ_1 .

We describe an extremely simple morphing algorithm for planar graphs, which simultaneously obtains properties of two earlier approaches: Floater and Gotsman’s barycentric interpolation method [30,32,58–60] results in morphs that are natural and visually appealing but are represented implicitly; variations on Cairns’ edge-collapse method [1,9,10,42,61] result in efficient explicit representations of morphs that are not useful for visualization. Our new algorithm efficiently computes an explicit piecewise-linear representation of a morph between drawings of the same 3-connected planar graph, that are potentially more useful for visualization than morphs based on Cairns’ method.

We also extend Floater and Gotsman’s planar morphing algorithm to geodesic graphs on the flat torus. Recent results of Luo, Wu, and Zhu [48] imply that Floater and Gotsman’s method directly generalizes to morphs between geodesic triangulations on surfaces of negative curvature, but a direct generalization to the torus generically fails [56]. Our extension is based on a simple scaling strategy, and it yields more natural morphs than previous algorithms based on edge collapses [12]. Finally, our arguments yield a straightforward proof of a conjecture of Connelly, Henderson, Ho, and Starbird [18] on the structure of the deformation space of geodesic triangulations of the torus.

1.1 Related Work

1.1.1 Planar Morphs

The history of morphing arguably begins with Steinitz [57, p. 347], who proved that any 3-dimensional convex polyhedron can be continuously deformed into any other convex polyhedron with the same 1-skeleton.

Cairns [9,10] was the first to prove the existence of morphs between arbitrary equivalent planar straight-line triangulations, using an inductive argument based on the idea of collapsing an edge from a low-degree vertex to one of its neighbors. Thomassen [61] extended Cairns’ proof to arbitrary planar straight-line graphs. Cairns and Thomassen’s proofs are constructive, but yield morphs consisting of an exponential number of steps.

Floater and Gotsman [30] proposed a more direct method to construct morphs between planar drawings, based on an extension by Floater [28] of Tutte’s classical spring embedding theorem [64]. Let Γ be a planar crossing-free straight-line drawing of a planar graph G , such that the boundary of every face of Γ is a strictly convex polygon, meaning the interior angle at every vertex is strictly less than π . We formally consider each edge of G to be a pair of oppositely directed half-edges or *darts*. Then every interior vertex in Γ is a strict convex combination of its neighbors; that is, we can associate a positive weight $\lambda_{u \rightarrow v}$ with each dart $u \rightarrow v$ in G , such that the vertex positions p_u in Γ satisfy the linear system

$$\sum_{u \rightarrow v} \lambda_{u \rightarrow v} (p_v - p_u) = (0, 0) \quad \text{for every interior vertex } u; \quad (1)$$

we emphasize that the sum is over the darts *leaving* u . Floater [28] proved that given arbitrary¹ positive weights $\lambda_{u \rightarrow v}$ and an arbitrary convex outer face, solving linear system (1) yields a straight-line drawing of G with convex faces. Tutte’s original spring-embedding theorem [64] is the special case of this result where every dart has weight 1, but his proof extends verbatim to arbitrary *symmetric* weights, where $\lambda_{u \rightarrow v} = \lambda_{v \rightarrow u}$ for every edge uv [39, 54, 62].

Floater and Gotsman [30] construct a morph between two convex drawings of the same planar graph G , with the same outer face, by linearly interpolating between weights $\lambda_{u \rightarrow v}$ consistent with the initial and final drawings. Suppose the input graph G has n vertices. Appropriate initial and final weights can be computed in $O(n)$ time using, for example, Floater’s mean-value coordinates [29, 40] or an averaging scheme also proposed by Floater [27, 30]. The resulting morphs are natural and visually appealing. However, the motions of the vertices are only computed implicitly; vertex positions at any time can be computed in $O(n^{\omega/2})$ time by solving a linear system via nested dissection [4, 45], where $\omega < 2.37286$ is the matrix multiplication exponent [3, 44].² Gotsman and Surazhsky generalized Floater and Gotsman’s technique to arbitrary planar straight-line graphs [32, 58–60].

A long series of later works, culminating in a paper by Alamdari, Angelini, Barrera-Cruz, Chan, Da Lozzo, Di Battista, Frati, Haxell, Lubiw, Patrignani, Roselli, Singla, and Wilkinson [1], describe an efficient algorithm to construct planar morphs with explicit piecewise-linear vertex trajectories, all ultimately based on Cairns’ inductive edge-collapsing strategy. Given any two equivalent planar crossing-free straight-line drawings of the same n -vertex planar graph, the resulting algorithm constructs a morph consisting of $O(n)$ *unidirectional* morphing steps, in which all vertices move along parallel lines at fixed speeds. Thus, each vertex moves along a piecewise-linear path of complexity $O(n)$, and the entire morph has complexity $O(n^2)$. These results require several delicate arguments; in particular, to perturb the *pseudomorphs* defined by edge collapses and their reversals into true morphs. Recent results of Klemz [43] imply that this algorithm can be implemented to run in $O(n^2 \log n)$ time on an appropriate real RAM model of computation. The resulting morph contracts all vertices into an exponentially small neighborhood and then expands them again, so it is not useful for visualization.

Angelini, Da Lozzo, Frati, Lubiw, Patrignani, and Roselli [5] consider the setting of *convexity-preserving* morphs between convex drawings, wherein every face remains strictly convex throughout the morph. Kleist, Klemz, Lubiw, Schlipf, Staals, and Strash [42] consider morphing to convexify any 3-connected planar drawing; specifically, *convexity-increasing* morphs wherein any angle that becomes convex during the morph remains convex throughout the rest of the morph. Both describe algorithms that produce piecewise-linear morphs consisting of $O(n)$ steps, and that can be implemented to run in time $O(n^{1+\omega/2})$. (Klemz [43] conjectures that both running times can be improved to $O(n^2 \log n)$.) Combining these algorithms results in an alternative piecewise-linear morph between 3-connected planar drawings.

1.1.2 Toroidal Morphs

Until recently, very little was known about morphing on tori or other more complex surfaces.

Tutte’s spring-embedding theorem was generalized to simple triangulations of surfaces with non-positive curvature by Colin de Verdière [17] and independently by Hass and Scott [35]. Delgado-

¹Floater’s presentation assumes that $\sum_{u \rightarrow v} \lambda_{u \rightarrow v} = 1$ for every interior vertex v , but this assumption is unnecessary.

²By solving the underlying linear system symbolically, it is possible to express the motion of each vertex as a rational function of degree $n - 1$, but computing vertex coordinates at any particular time from this representation requires $O(n^2)$ time.

Friedrichs [22], Lovász [46], and Gortler, Gotsman, and Thurston [31] also independently proved an extension of Tutte’s theorem to graphs on the flat torus whose universal covers are simple and 3-connected. For any toroidal graph and any assignment of positive *symmetric* weights to the darts, solving a linear system similar to (1) yields vertex positions of a geodesic drawing with strictly convex faces [25, 31]; see Section 2 for details. Thus, if two isotopic toroidal crossing-free geodesic drawings Γ_0 and Γ_1 can both be described by symmetric dart weights, linearly interpolating those weights yields a morph from Γ_0 to Γ_1 [16]; in light of the authors’ toroidal Maxwell–Cremona correspondence [25], this can be seen as a natural toroidal analogue of Steinitz’s theorem on morphing convex polyhedra [57].

The restriction to symmetric weights is both nontrivial and significant. In a toroidal crossing-free geodesic drawing with (strictly) convex faces, every vertex can be described as a convex combination of its neighbors, but not necessarily with symmetric weights. Moreover, the linear system expressing vertex positions as convex combinations of its neighbors is rank-deficient, and therefore is not solvable in general; see Appendix A for an example. Thus, Floater’s asymmetric extension of Tutte’s theorem does *not* directly generalize to the flat torus.

For similar reasons, Floater and Gotsman’s planar morphing algorithm also does not generalize. Suppose we are given two isotopic toroidal crossing-free geodesic drawings Γ_0 and Γ_1 , each with dart weights that express their vertices as convex combinations of their neighbors. Unfortunately, in general, interpolating those weights yields linear systems that have no solution; we give a simple example in Appendix A.

Steiner and Fischer [56] modify the system by fixing a single vertex, restoring full rank. However, solving the modified system does not necessarily yield a crossing-free drawing, because the fixed vertex may not lie in the convex hull of its neighbors.³ Moreover, even though the initial and final weights are consistent with crossing-free drawings, averages of those weights may not be. We give an example of this bad behavior in Appendix A.

Chambers, Erickson, Lin, and Parsa [12] described the first algorithm to morph between arbitrary essentially 3-connected toroidal crossing-free geodesic drawings. Their algorithm uses a combination of Cairns’ edge-collapsing strategy and spring embeddings to construct a morph consisting of $O(n)$ unidirectional morphing steps, in $O(n^{1+\omega/2})$ time. Like planar morphs built from edge collapses, these toroidal morphs contract vertices into small neighborhoods and thus are not suitable for visualization.

Recently, Luo, Wu, and Zhu [48] generalized Floater’s theorem to geodesic triangulations of arbitrary closed Riemannian 2-manifolds with strictly negative curvature, extending the spring-embedding theorems of Colin de Verdière [17] and Hass and Scott [35] to asymmetric weights. Their result immediately implies that if two geodesic triangulations of such a surface are homotopic, then linearly interpolating the dart weights yields a continuous family of crossing-free geodesic drawings, or in other words, a morph. Their result applies only to surfaces with negative Euler characteristic; alas, the torus has Euler characteristic 0.

1.2 New Results

We describe two applications of Floater and Gotsman’s barycentric interpolation strategy, which yield simpler algorithms for planar and toroidal morphing.

First we describe a very simple algorithm to construct piecewise-linear morphs between planar crossing-free straight-line drawings. Given two equivalent planar straight-line crossing-free straight-

³Steiner and Fischer incorrectly claim [56, Section 2.2.1] that the resulting drawing has no “foldovers” except at the fixed vertex and its neighbors; see Appendix A.

line drawings Γ_0 and Γ_1 with strictly convex faces and the same outer face, we construct a morph from Γ_0 to Γ_1 that consists of $O(n)$ unidirectional morphing steps, in $O(n^{1+\omega/2})$ time. Our morphing algorithm computes barycentric weights for the darts in Γ_0 and Γ_1 in a preprocessing phase, and then for each morphing step, interpolates only the pair of weights associated with a single edge. Our key observation is that changing the weights for a single edge e moves all vertices in the Floater drawing along lines parallel to e , implying that interpolation corresponds to a unidirectional morph. (The same observation was made for *symmetric* edge weights by Chambers *et al.* [12].) Our algorithm is significantly simpler than that of Angelini *et al.* [5] for computing convexity-preserving morphs. We then extend our algorithm to drawings with non-convex faces, using a simple alternative approach to that of Kleist *et al.* [42]. Figure 1 shows a morph computed by our algorithm; in each frame, the weights of the bold red edge are about to change.

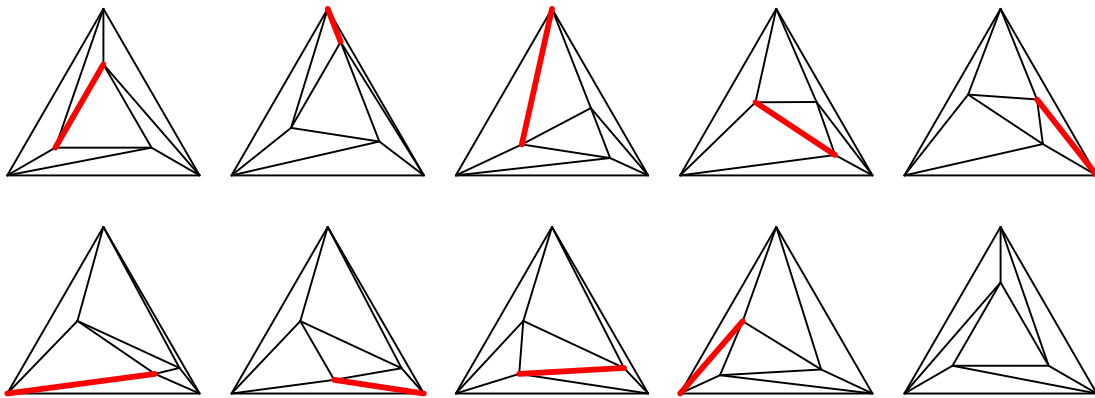


Figure 1: Incrementally morphing between planar graphs.

Next, we describe a natural extension of Floater and Gotsman’s method to geodesic drawings on the flat torus. Our key observation is that barycentric dart weights can be *scaled* so that barycentric interpolation works. Specifically, we call a weight assignment *morphable* if every *column* of the resulting Laplacian linear system sums to zero; averages of morphable weights are morphable. Given any weight assignment consistent with any convex drawing, we can guarantee morphability by scaling the weights of all darts leaving each vertex v —or equivalently, scaling each *row* of the linear system—by a common positive scalar α_v . This scaling obviously has no effect on the solution space of the system. Positivity of the scaling vector α follows from a weighted directed version of the matrix-tree theorem [8, 20, 63], or from the Perron-Frobenius theorem [14]. We can compute the appropriate scaling in $O(n^{\omega/2})$ time, after which we can compute any intermediate drawing in $O(n^{\omega/2})$ time, matching the performance of Floater and Gotsman exactly. The resulting morphs are natural and visually appealing, and our proofs of correctness are considerably simpler than those of Chambers *et al.* [12]. However, unlike Chambers *et al.*, our new morphing algorithm does not compute explicit vertex trajectories. Figure 2 shows a morph computed by our algorithm between two randomly shifted 6×6 toroidal grids. (The authors’ Python implementation is available on request.)

It remains an open question whether our results can be combined to compute explicit low-complexity piecewise-linear toroidal morphs without edge collapses. We offer some preliminary observations in Appendix B.

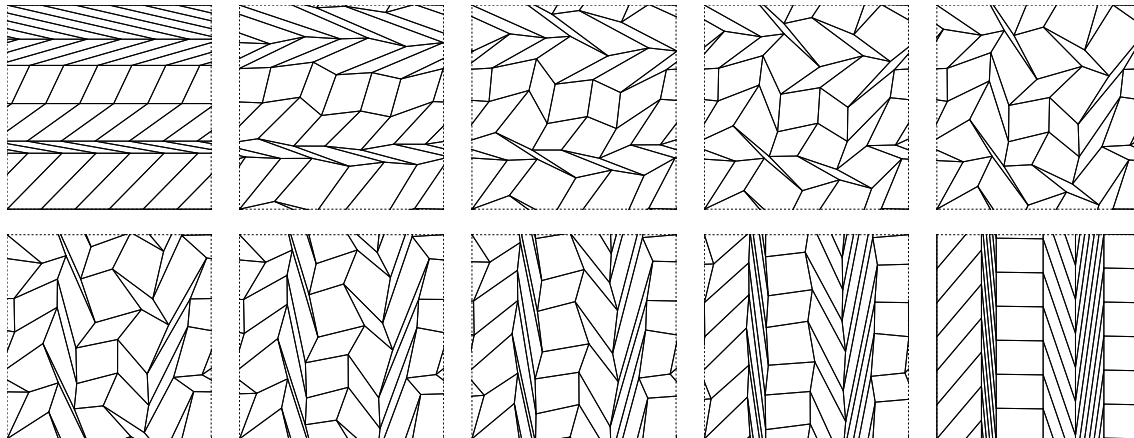


Figure 2: Morphing between randomly shifted toroidal grids.

2 Definitions and Notation

2.1 Plane Graphs

Any planar straight-line drawing Γ of an n -vertex graph can be represented by a *position* matrix $P \in \mathbb{R}^{n \times 2}$, each row p_v of which gives the location of some vertex v . Thus, each edge uv is drawn as the straight-line segment $p_u p_v$. We call a planar drawing *convex* if it is crossing-free, every bounded face is a strictly convex polygon, and the outer face is the complement of a strictly convex polygon.

Formally, we regard each edge of any graph as a pair of opposing half-edges or *darts*, each directed from its *tail* to its *head*. We write $\text{rev}(d)$ to denote the reversal of any dart d . For simple graphs, we write $u \rightarrow v$ to denote the dart with tail u and head v . A *barycentric weight vector* for Γ assigns a positive real number $\lambda_{u \rightarrow v}$ to every dart $u \rightarrow v$ of a graph, so that the vertex positions p_v satisfy Floater's linear system (1). Conversely, for a fixed graph G with a fixed strictly convex outer face, the *Floater drawing* Γ^λ of G with respect to a positive weight vector λ is the unique drawing whose vertex positions p_v satisfy system (1). We call a weight vector λ *symmetric* if $\lambda_d = \lambda_{\text{rev}(d)}$ for every dart d .

A *morph* between two planar drawings Γ_0 and Γ_1 is a continuous family of crossing-free drawings Γ_t parametrized by time, starting at Γ_0 and ending at Γ_1 . A morph is *linear* if each vertex moves along a straight line at constant speed, and *piecewise-linear* if it is the concatenation of linear morphs. Any piecewise-linear morph can be described by a finite sequence of straight-line drawings, or their position matrices. A linear morph is *unidirectional* if vertices move along parallel lines.

2.2 Torus Graphs

The *flat torus* is the quotient space $\mathbb{T} = \mathbb{R}^2 / \mathbb{Z}^2$, also obtained by identifying opposite sides of the unit square $[0, 1]^2$. A *geodesic* on the flat torus is the image of a line segment in \mathbb{R}^2 under the

projection map $\pi: \mathbb{R}^2 \rightarrow \mathbb{T}$ where $\pi(x, y) = (x \bmod 1, y \bmod 1)$.⁴

A (crossing-free) *geodesic torus drawing* Γ of a graph G maps its vertices to distinct points in \mathbb{T} and its edges to simple, interior-disjoint geodesics. We explicitly consider geodesic drawings of graphs with loops and parallel edges. We write $d: u \rightarrow v$ to declare that d is a dart with tail u and head v ; we emphasize that (unlike in planar setting) there may be more than one such dart; see Figure 3 for an example.

Every geodesic torus drawing Γ of a graph G is the projection of an infinite, doubly-periodic planar straight-line graph $\tilde{\Gamma}$, called the *universal cover* of Γ [12]; see Figure 3 for an example. We call Γ *essentially simple* if its universal cover $\tilde{\Gamma}$ is simple, and *essentially 3-connected* if $\tilde{\Gamma}$ is 3-connected [50, 51]. Finally, we call Γ a *convex* drawing if every face of $\tilde{\Gamma}$ is strictly convex. Every convex torus drawing is both essentially simple and essentially 3-connected, since every infinite planar graph with strictly convex faces is 3-connected [21].

Coordinate representations. Following Chambers *et al.* [12], we use a *coordinate representation* (P, τ) for geodesic torus drawings that records

- a *position* vector $p_v \in \mathbb{R}^2$ for each vertex v , and
- a *translation* vector $\tau_d \in \mathbb{Z}^2$ for each dart d , such that $\tau_{rev(d)} = -\tau_d$.

These vectors indicate that each dart $d: u \rightarrow v$ is drawn as the projection of a line segment from p_u to $p_v + \tau_d$ in the universal cover $\tilde{\Gamma}$. In particular, if we normalize all vertex positions to the half-open unit square $[0, 1)^2$, then each translation vector τ_d indicates the number of times d crosses the vertical boundary of the unit square to the right, and the number of times d crosses the horizontal boundary of the unit square upward. In practice, however, such normalization is not necessary.

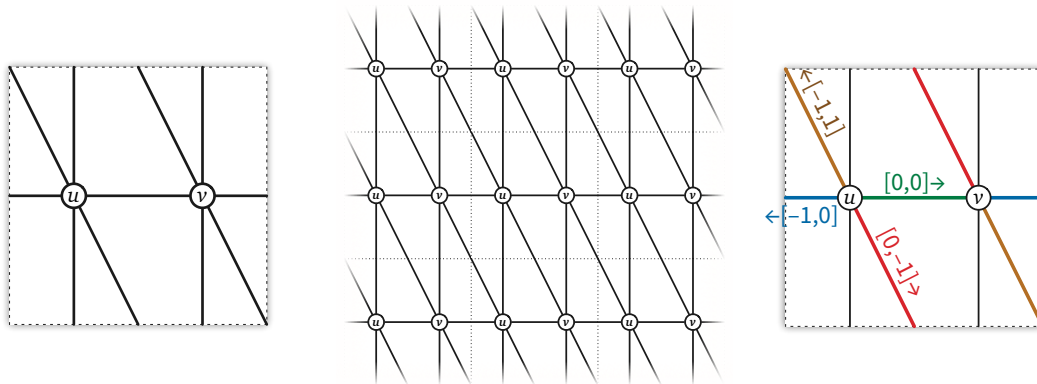


Figure 3: A crossing-free geodesic torus drawing, its universal cover, and translation vectors for the four darts from u to v . The graph also contains loops at u and at v .

Two crossing-free drawings of the same graph on the flat torus are *isotopic* if one can be deformed into the other through a continuous family of (not necessarily geodesic) crossing-free

⁴Identifying opposite sides of any other parallelogram yields a different flat torus; all flat tori are related by homeomorphisms induced by linear transformations that map geodesics to geodesics, and therefore map morphs to morphs. Thus, like Chambers *et al.* [12], our results also automatically apply to crossing-free geodesic drawings on *any* flat torus.

drawings; such a deformation is called an *isotopy*. Two crossing-free *geodesic* drawings are isotopic if and only if their coordinate representations can be *normalized* so that their translation vectors agree; this condition can be tested in $O(n)$ time [12, Theorem A.1], [15] where, as usual, n is the number of vertices. A *geodesic isotopy* or *morph* is an isotopy in which all intermediate drawings are geodesic.

Barycentric weights. In any convex toroidal drawing Γ , the position p_v of each vertex v can be expressed as a convex combination of its neighbors, as follows. We can assign a weight $\lambda_d > 0$ to each dart d such that any coordinate representation (P, τ) of Γ satisfies the linear system

$$\sum_v \sum_{d:u \rightarrow v} \lambda_d (p_v - p_u + \tau_d) = (0, 0) \quad \text{for every vertex } u. \quad (2)$$

Note that since we explicitly allow self-loops, there may be darts $d : u \rightarrow u$ that contribute a value of $\lambda_d \tau_d$ to this sum.

We can express this linear system in matrix notation as $L^\lambda P = H^\lambda$, where

$$L_{ij}^\lambda = \begin{cases} \sum_k \sum_{d:i \rightarrow k} \lambda_d & \text{if } i = j \\ \sum_{d:i \rightarrow j} -\lambda_d & \text{otherwise} \end{cases} \quad \text{and} \quad H_i^\lambda = \sum_j \sum_{d:i \rightarrow j} \lambda_d \tau_d \quad (2')$$

The (unnormalized, asymmetric) Laplacian matrix L^λ has rank $n - 1$ [56]. We call any positive weight vector λ satisfying system (2) *barycentric* for Γ . Barycentric weights for any convex torus drawing can be computed in $O(n)$ time using, for example, Floater's mean-value coordinates [29, 40].

On the other hand, suppose we fix the graph G and translation vectors τ_d consistent with an essentially 3-connected drawing of G . Then for any positive weight vector λ , any solution to linear system (2) gives the vertex positions p_v of a convex drawing Γ^λ of G [31]. In this case, we say that the *Floater drawing* Γ^λ *realizes* the weight vector λ , and we call the weight vector λ *realizable* for the graph G . Every realizable weight vector is realized by a two-dimensional family of drawings that differ by translation.

Every *symmetric* positive weight vector (where $\lambda_d = \lambda_{rev(d)}$) is realizable: for any assignment of positive weights to the *edges* of G , there is a corresponding convex torus drawing [17, 22, 31, 35, 46]. Realizable weights are not necessarily symmetric: there are convex torus drawings with only asymmetric barycentric weights. Conversely, positive asymmetric weights are not always realizable.

3 Morphing Plane Graphs Edge by Edge

Fix a 3-connected planar graph G . Suppose we want to morph between two crossing-free straight-line drawings of G with the same convex outer face. We describe a very simple algorithm to morph between such drawings that combines the benefits of both the Floater and Gotsman approach [30, 32, 58–60] and the Cairns approach [1, 9, 10, 42, 61]. Specifically, our algorithm constructs a morph consisting of $O(n)$ unidirectional morphing steps, in $O(n^{1+\omega/2})$ time; moreover, because our morphs do not use edge collapses, they are potentially good for visualization.

Some of our planar morphing algorithms rely on a slight generalization of Floater's embedding theorem [28] that allows some darts to have weight zero. For any non-negative weight vector λ , let G_λ denote the directed graph induced by darts of G whose weights are positive. Recall that

a directed graph is *strongly 3-connected* if there are at least three vertex-disjoint paths from any vertex to any other vertex, or equivalently by Menger’s theorem, if deleting any two vertices leaves a strongly connected subgraph.

Theorem 1 *Let G be a planar graph with a fixed, strictly convex outer face, and let λ be an assignment of non-negative weights to the darts of G . If the directed graph G_λ induced by positive darts is strongly 3-connected, then linear system (1) has a unique solution, which describes a convex drawing of G .*

Theorem 1 follows immediately from a similar theorem of Haas, Order, Rote, Santos, Servatius, Servatius, Souvaine, Streinu, and Whiteley [34, Theorem 8], which uses a weaker connectivity condition.

Let p_v^λ denote the position of vertex v in the Floater drawing Γ^λ of G with respect to weight vector λ . The following key lemma is a planar asymmetric version of Lemma 5.1 of Chambers *et al.* [12]. Intuitively, it states that changing the weights of the darts of a single edge e moves each vertex in the Floater drawing along lines parallel to e .

Lemma 1 *Let G be a 3-connected planar graph with a fixed, strictly convex outer face. Let λ and μ be arbitrary non-negative weight vectors such that the directed graphs G_λ and G_μ are strongly 3-connected. Suppose $\lambda_d \neq \mu_d$ or $\lambda_{rev(d)} \neq \mu_{rev(d)}$ for some dart d , but $\lambda_{d'} = \mu_{d'}$ for all darts $d' \notin \{d, rev(d)\}$. Then for each interior vertex w , the vector $p_w^\mu - p_w^\lambda$ is parallel to the drawing of d in Γ^λ .*

Proof: Theorem 1 implies that the Floater drawings Γ^λ and Γ^μ are well-defined convex drawings of G .

Suppose d has tail u and head v , and (by rotating the drawing if necessary) that d is drawn parallel to the x -axis. For each vertex i , let y_i^λ and y_i^μ be the y -coordinates of points p_i^λ and p_i^μ , respectively. In particular, that $y_u^\lambda = y_v^\lambda$. We need to prove that $y_w^\lambda = y_w^\mu$ for every vertex w .

Projecting linear system (1) for λ onto the y -axis gives us

$$\sum_{i \rightarrow j} \lambda_{i \rightarrow j} (y_j^\lambda - y_i^\lambda) = 0 \quad \text{for each interior vertex } i. \tag{3}$$

Swapping entries of λ with corresponding entries of μ in the system (3) changes at most two constraints, corresponding to the two endpoints u and v of d . Moreover, in each changed constraint, the single changed coefficient is multiplied by $y_u^\lambda - y_v^\lambda = y_v^\lambda - y_u^\lambda = 0$, so the y_i^λ ’s also solve the corresponding system for μ . Since the system (3) and its counterpart for μ each have a unique solution [34], we conclude that $y_w^\lambda = y_w^\mu$ for every vertex w . □

3.1 Morphing Convex Drawings

We make use of the following lemma:

Lemma 2 (Chambers *et al.* [12, Lemma 5.2]) *Let p_0p_1 , q_0q_1 , and r_0r_1 be arbitrary parallel segments in the plane. For all real $0 \leq t \leq 1$, define $p_t = (1 - t)p_0 + tp_1$ and $q_t = (1 - t)q_0 + tq_1$ and $r_t = (1 - t)r_0 + tr_1$. If the triples p_0, q_0, r_0 and p_1, q_1, r_1 are oriented counterclockwise, then for all $0 \leq t \leq 1$, the triple p_t, q_t, r_t is also oriented counterclockwise.*

Under the assumptions of Lemma 1, consider the intermediary drawings resulting from linearly interpolating vertex positions from Γ^λ to Γ^μ . Applying Lemma 2 to each angle in the initial and final drawings implies that the angle maintains its orientation in all the intermediary drawings. In other words, no crossings can be introduced—all intermediate drawings are crossing-free. Put more simply, linear interpolation of vertex positions from Γ^λ to Γ^μ yields a unidirectional linear morph. (Alamdari *et al.* used a similar observation [1, Corollary 7.2].)

It follows that we can derive a planar morph between equivalent *convex* drawings through a sequence of at most $3n-9$ unidirectional linear morphing steps, one for each internal edge, using the algorithm in Figure 4. Initial and final barycentric weight vectors can be found in $O(n)$ time using, for example, Floater’s mean-value method [29, 40]. Each intermediate drawing can be computed in $O(n^{\omega/2})$ time using nested dissection [4, 45], for a total running time of $O(n^{1+\omega/2})$.

| |
|-----------------------------------------------------------------------------------------------------------------------------------------------------------------------------------------------------------------------------------------------------------------------------------------------------------------------------------------------------------------------------------------------------------------------------------------------------------------------------------------------------------------------------------------------------------------------------------------------------------------------------------------------------------------------------------------------------------------------------------------------------------|
| <pre> MORPHCONVEX($\Gamma_{\text{start}}, \Gamma_{\text{end}}$): $\lambda \leftarrow$ barycentric weights for Γ_{start} $\mu \leftarrow$ barycentric weights for Γ_{end} $k \leftarrow 0$ for each internal edge e $k \leftarrow k + 1$ $d \leftarrow$ a dart of e $\lambda_d \leftarrow \mu_d$ $\lambda_{\text{rev}(d)} \leftarrow \mu_{\text{rev}(d)}$ $\Gamma_k \leftarrow \Gamma^\lambda$ return $\Gamma_{\text{start}}, \Gamma_1, \Gamma_2, \dots, \Gamma_k$ $\langle\langle = \Gamma_{\text{end}} \rangle\rangle$ </pre> |
|-----------------------------------------------------------------------------------------------------------------------------------------------------------------------------------------------------------------------------------------------------------------------------------------------------------------------------------------------------------------------------------------------------------------------------------------------------------------------------------------------------------------------------------------------------------------------------------------------------------------------------------------------------------------------------------------------------------------------------------------------------------|

Figure 4: Algorithm for morphing between convex planar drawings.

Because all Floater drawings are convex, the planar morph produced by MORPHCONVEX is actually a *convexity-preserving* piecewise-linear planar morph; all faces remain convex throughout the morph. The existence of convexity-preserving morphs was first proved by Thomassen [61]; Angelini, Da Lozzo, Frati, Lubiw, Patrignani, and Roselli [5] described a piecewise-linear convexity-preserving morph consisting of $O(n)$ steps. Our algorithm is significantly simpler than that of Angelini *et al.* [5].

Theorem 2 *Given any two equivalent convex planar drawings with n vertices and the same convex outer face, we can compute a morph between them consisting of at most $3n-9$ unidirectional linear morphing steps, in $O(n^{1+\omega/2})$ time.*

3.2 Morphing Non-convex Drawings

We can extend the previous algorithm to non-convex drawings, by morphing through intermediate convex drawings, using a similar edge-by-edge method. Specifically, we morph any 3-connected planar crossing-free straight-line drawing Γ with a convex outer face into an equivalent convex drawing, as shown in the CONVEXIFY method as shown in Figure 5.

First, we add edges to Γ to decompose its interior faces into convex polygons, for example by triangulating every face, and compute barycentric weights for the resulting convex drawing K . Let H denote the underlying graph of K . Then, one by one, for each added edge e , we reduce the weights of e to zero and compute a new Floater drawing of H . Because the input graph G is 3-connected, the directed graph induced by the positive darts of H is always strongly 3-connected;

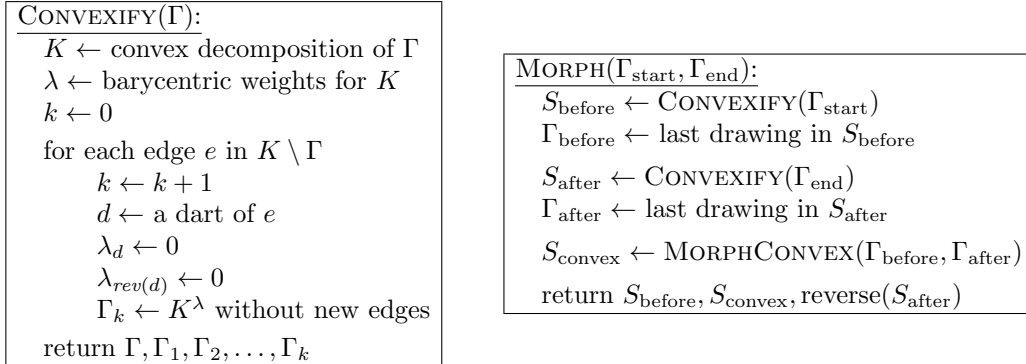


Figure 5: Algorithm for morphing between general planar straight-line drawings.

thus, in each iteration, Theorem 1 implies that the resulting Floater drawing K^λ is a convex drawing of H .⁵ Again, each Floater drawing K^λ can be computed in $O(n^{\omega/2})$ time. Dropping the added edges yields a sequence of convex drawings $\Gamma_1, \Gamma_2, \dots, \Gamma_k$, all equivalent to Γ and with the same outer face. Lemmas 1 and 2 imply that for each index j , linearly interpolating vertex positions from Γ_{j-1} to Γ_j yields a unidirectional linear morph; concatenating these unidirectional linear morphing steps yields a morph from Γ to the final convex drawing Γ_k .

Because the input graph G is 3-connected, every vertex has degree at least 3, so G has at least $1.5n$ edges. On the other hand, Euler’s formula implies that our initial and final convex decompositions have at most $3n - 6$ edges, and therefore at most $3n - 9$ internal edges. Thus, each of our convex decompositions requires at most $1.5n - 6$ additional edges. Let x be the maximum number of additional edges needed in either convex decomposition. In this case G can have at most $3n - 9 - x$ internal edges, and so our morph consists of at most $x + (3n - 9 - x) + x = 3n - 9 + x \leq 4.5n - 15$ unidirectional linear morphing steps. In summary:

Theorem 3 *Given any two equivalent 3-connected planar crossing-free straight-line drawings with n vertices and the same convex outer face, we can compute a morph between them consisting of at most $4.5n - 15$ unidirectional linear morphing steps, in $O(n^{1+\omega/2})$ time.*

3.3 Convexity-Increasing Morphs

Our algorithm CONVEXIFY is arguably simpler than that of Kleist *et al.* [42], but unlike Kleist *et al.*, our algorithm is not necessarily *convexity-increasing*; it is possible for angles of interior faces to change from convex to reflex during the morph. A slightly more complex variant of our algorithm produces convexity-increasing morphs. At each iteration of the new algorithm, we explicitly set the weights of all diagonal darts inside any convex angle to zero and recompute the weights of all other darts from scratch; setting those diagonal dart weights to zero ensures that convex angles remain convex in future iterations.

We start by computing an arbitrary convex decomposition K of the input drawing Γ , for example by triangulating every face. We call the new edges in $K \setminus \Gamma$ *diagonals*.

We call a diagonal *redundant* if the union of the faces on either side is strictly convex, or equivalently, if its removal from the convex subdivision results in a convex subdivision; we can test

⁵In fact, setting the weight on both darts of e to zero has exactly the same effect on linear system (1) as deleting edge e from the graph, which means we can apply Floater’s theorem directly.

the redundancy of any diagonal in constant time. We can easily ensure that our initial convex decomposition K has no redundant diagonals [33, 37, 41], but as we morph K (and thus Γ), new diagonals will become redundant. Deleting a redundant edge leaves a coarser convex decomposition, but may also make some other redundant edges non-redundant. We call a diagonal dart $u \rightarrow v$ *irrelevant* if u lies inside a convex corner of some face of Γ ; we emphasize that the reversal of an irrelevant dart may not be irrelevant. A dart is *relevant* if it is not irrelevant.

Let H denote the underlying graph of the convex decomposition K . Our morphing algorithm changes the weights of some darts in H to zero, but only darts of diagonals; every dart of the input graph G has positive weight throughout the entire algorithm. As a result, the directed graph H_λ induced by positive-weight darts is always strongly 3-connected, which allows us to apply Theorem 1.

Let $K_0 = K$ be the initial convex decomposition of Γ , and let $\Gamma_0 = \Gamma$. For each positive integer k , the k th iteration of our algorithm proceeds as follows.

- Identify all irrelevant darts in the convex decomposition K_{k-1} computed in the previous iteration.
- Compute a barycentric weight vector μ_{k-1} for K_{k-1} by setting the weights of all irrelevant darts to zero, and computing weights for the *relevant* darts leaving each vertex using Floater's mean-value method [29, 40].
- Choose an arbitrary diagonal e_k in K_{k-1} , change the weights of both of its darts to zero, and compute a new Floater drawing K_k with respect to the resulting weight vector λ_k . Theorem 1 implies that every face of K_k is strictly convex.
- Delete the (now redundant) diagonal e_k , and optionally any other redundant diagonals, from K_k .
- Finally, let Γ_k be the restriction of K_k to the original graph G .

Because the weight vectors μ_{k-1} and λ_k differ on exactly one edge, Lemmas 1 and 2 imply that linearly interpolating vertex positions from Γ_{k-1} to Γ_k yields a unidirectional linear morph. We emphasize that the weight vectors λ_k and μ_k are not necessarily equal, even though both are consistent with the drawing K_k . The running time of each iteration is dominated by the time to compute the Floater drawing K_k . Because every iteration decreases the number of diagonals, the number of iterations is $O(n)$, so the overall running time of our algorithm is still $O(n^{1+\omega/2})$.

It remains to argue that the resulting morph is convexity-increasing. Consider an arbitrary convex corner uvw of an arbitrary face of Γ_{k-1} . All diagonal darts in K_{k-1} that leave v inside the wedge bounded by $v \rightarrow u$ and $v \rightarrow w$ are irrelevant, and thus are given weight 0. In the new drawing K_k , vertex v is a weighted average of its out-neighbors in the directed graph induced by positive-weight darts. Because darts $v \rightarrow u$ and $v \rightarrow w$ have positive weights, it follows that corner uvw is convex in Γ_k . Finally, Lemmas 1 and 2 imply that this corner remains convex as we interpolate vertices from Γ_{k-1} to Γ_k .

Theorem 4 *Given any 3-connected planar straight-line drawing with n vertices and a convex outer face, we can compute a convexity-increasing morph to an equivalent convex planar drawing with the same outer face, consisting of at most $1.5n - 6$ unidirectional linear morphing steps, in $O(n^{1+\omega/2})$ time.*

3.4 Remarks on the Model of Computation

The algorithm of Alamdari *et al.* [1] requires a slightly nonstandard real RAM model of computation that supports exact square and exact cube roots. In contrast, Floater’s mean-value weights can be expressed in terms of areas and Euclidean lengths [40], which require only square roots to evaluate exactly. If initial and final barycentric weights are given, both Floater and Gotsman’s morphing algorithm [30] and our incremental algorithm use only basic arithmetic operations: addition, subtraction, multiplication, and division.

Even without exact roots, any integer-RAM or floating-point implementation of our morphing algorithm must contend with precision issues. A careful implementation of Alon and Yuster’s nested dissection algorithm [4] solves Floater’s linear system (1) exactly in $O(n^{1+\omega/2} \text{polylog } n)$ bit operations, assuming all dart weights $\lambda_{u \rightarrow v}$ are $O(\log n)$ -bit integers [4, 6]. Thus, at least when all weights are given as part of the input, an exact implementation of our morphing algorithm runs in $O(n^{2+\omega/2} \text{polylog } n)$ on a standard integer RAM. Coordinates of Tutte/Floater drawings can require $\Omega(n)$ bits of precision to avoid collapsing or crossing edges [23, 24]; a canonical bad example is shown in Figure 6. Thus, the near-linear cost of exact arithmetic is unavoidable in the worst case.

Shen, Jiang, Zorin, and Panozzo [55] observe that floating-point implementations of Tutte’s algorithm suffer from robustness issues in practice. Shen *et al.* describe an iterative procedure to repair floating-point-Tutte drawings; however, it is unclear whether a similar procedure can be used to avoid precision issues in our algorithm while maintaining continuity of the resulting morph. It is also unclear whether precision issues in our algorithm can be avoided, or at least minimized, by carefully choosing the order in which edge weights are changed and/or by morphing through a carefully chosen intermediate drawing.

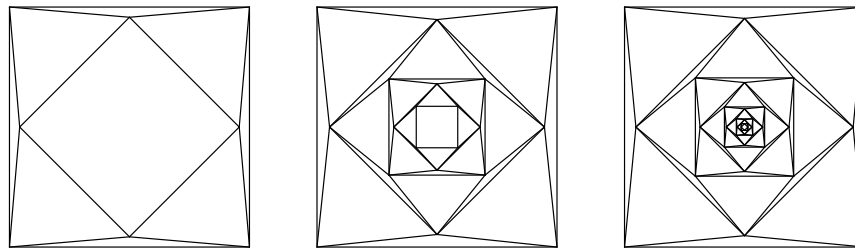


Figure 6: A family of weighted Floater drawings consisting of nested squares, with 2, 5, and 10 layers, respectively.

4 Morphable Weight Vectors on the Flat Torus

As observed by Steiner and Fischer [56], Floater and Gotsman’s morphing algorithm does not directly generalize to the toroidal setting, since not all positive weight vectors λ are realizable. In particular, given arbitrary barycentric weights $\lambda(0)$ and $\lambda(1)$ of two isotopic convex torus drawings, intermediate weights $\lambda(t) := (1 - t)\lambda(0) + t\lambda(1)$ are not necessarily realizable; see Appendix A for an example. Thus, interpolating barycentric weights does not necessarily give us a morph.

To bypass this issue, we identify a subspace of weight vectors, which we call *morphable*, such that every convex torus drawing has a morphable barycentric weight vector, every morphable weight

vector is realizable, and convex combinations of morphable weights are morphable. Specifically, a positive weight vector λ is *morphable* if each *column* of the matrices L^λ and H^λ sums to 0.⁶ The following lemma is immediate:

Lemma 3 *Convex combinations of morphable weight vectors are morphable.*

Lemma 4 *Every morphable weight vector is realizable.*

Proof: If λ is a morphable weight vector, then the n th row of the linear system $L^\lambda P = H^\lambda$ is implied by the other $n - 1$ rows, so we can remove it. The resulting abbreviated linear system still has rank $n - 1$, so it has a (unique) solution. \square

Lemma 5 *Every symmetric weight vector is morphable.*

Proof: For every weight vector λ , each *row* of the Laplacian matrix L^λ sums to zero. If the weight vector λ is symmetric, then the matrix L^λ is also symmetric, so its columns also sum to zero. On the other hand, if λ is symmetric, then the linear system $L^\lambda P = H^\lambda$ is solvable [31], which implies that the columns of H^λ also sum to zero. \square

Lemma 6 *Given a barycentric weight vector λ for a convex torus drawing Γ , a morphable barycentric weight vector for Γ can be computed in $O(n^{\omega/2})$ time.*

Proof: The matrix L^λ has rank $n - 1$, so there is a one-dimensional space of (row) vectors $\alpha = (\alpha_1, \dots, \alpha_n)$ such that $\alpha L^\lambda = (0, \dots, 0)$. We can compute a non-zero vector α in $O(n^{\omega/2})$ time using nested dissection [2, 4, 45].

We will show that we can choose all α_i to be positive; since the space of solutions α is one-dimensional, any such α we compute must have entries of all the same sign and thus we can assume positivity by multiplying by -1 if necessary. Our proof that all α_i can be chosen to be positive will be by a directed version of the matrix tree theorem [8, 20, 63]; see also Cohen *et al.* [14, Lemma 1] for an alternate proof using the Perron-Frobenius theorem. Let G^\pm be the weighted directed graph whose weighted arcs correspond to the weighted darts of the underlying graph G of Γ . An *inward directed spanning tree* is an acyclic spanning subgraph of G^\pm where every vertex except one (called the *root*) has out-degree 1. The weight of an inward directed spanning tree is the product of the weights of its arcs. For each i , let α_i be the sum of the weights of all inward directed spanning trees rooted at vertex i ; we have $\alpha_i > 0$ because all dart weights are positive. The directed matrix tree theorem implies that $\alpha L = 0$, as required; for an elementary proof, see De Leenheer [20, Theorem 3].

Define a new weight vector μ by setting $\mu_d := \alpha_{tail(d)} \lambda_d$ for each dart d . For each index i , we immediately have $L_i^\mu P = \alpha_i L_i^\lambda P = \alpha_i H_i^\lambda = H_i^\mu$, where P is the position matrix for Γ , so μ is in fact a barycentric weight vector for Γ . Finally, we observe that $(1, \dots, 1)L^\mu = \alpha L^\lambda = (0, \dots, 0)$ and $(1, \dots, 1)H^\mu = \alpha H^\lambda = \alpha L^\lambda P = (0, \dots, 0)P = (0, 0)$, which imply that μ is morphable. \square

Theorem 5 *Given coordinate representations of two isotopic essentially 3-connected toroidal crossing-free geodesic drawings Γ_0 and Γ_1 , we can efficiently compute a morph from Γ_0 to Γ_1 . Specifically, after $O(n^{\omega/2})$ preprocessing time, we can compute any intermediate drawing during the morph in $O(n^{\omega/2})$ time.*

⁶Directed graph Laplacians whose columns sum to zero are also called *Eulerian*; Cohen *et al.* [14] refer to the scaling process described by Lemma 6 as *Eulerian scaling*.

Proof: Suppose Γ_0 and Γ_1 are convex drawings. First, if necessary, we normalize the given coordinate representations so that their translation vectors agree, in $O(n)$ time [12, Theorem A.1]. Then we find barycentric weight vectors $\lambda(0)$ and $\lambda(1)$ for Γ_0 and Γ_1 , respectively, in $O(n)$ time, for example using Floater’s mean-value coordinates [29, 40]. Following Lemma 6, we derive morphable weights $\mu(0)$ and $\mu(1)$ from $\lambda(0)$ and $\lambda(1)$, respectively, in $O(n^{\omega/2})$ time. Finally, given any real number $0 < t < 1$, we set $\mu(t) := (1 - t)\mu(0) + t\mu(1)$ and solve the linear system $L^{\mu(t)}P^{(t)} = H^{\mu(t)}$ for the position matrix $P^{(t)}$ of an intermediate drawing $\Gamma^{\mu(t)}$; Lemmas 3 and 4 imply that this system is solvable. The function $t \mapsto \Gamma^{\mu(t)}$ is a convexity-preserving morph between Γ_0 and Γ_1 .

If the faces of Γ_0 or Γ_1 are not convex, we morph through an intermediate convex drawing, similarly to Chambers *et al.* [12, Theorem 8.1]. Let Γ_* be the Floater drawing of G obtained by setting every dart weight to 1. Compute any triangulation T_0 of Γ_0 , and then triangulate the convex faces Γ_* using the same diagonals, to obtain a triangulation T_* isotopic to T_0 . Assign weight 0 to the darts of the diagonals in $T_* \setminus \Gamma_*$ to obtain a barycentric weight vector μ_* for T_* , which is symmetric and therefore morphable, by Lemma 5. Derive morphable weights μ_0 for T_0 using mean-value coordinates [29, 40] and Lemma 6. Then we can morph from T_0 to T_* by weight interpolation, using the weight vector $\mu(t) := (1 - 2t)\mu_0 + 2t\mu_*$ for any $0 \leq t \leq 1/2$. Ignoring the diagonal edges gives us a morph from Γ_0 to Γ_* . A symmetric procedure yields a morph from Γ_* to Γ_1 . □

4.1 Deformation Space of Geodesic Torus Drawings

Our techniques also imply a stronger theorem about the space of all crossing-free geodesic drawings in a particular isotopy class on the flat torus. Before we describe the result, we need to recall some basic definitions from topology. For further topology background, we refer the reader to Hatcher [36] or Munkres [52].

Let X and Y be arbitrary topological spaces. A *homotopy* between two continuous functions $f: X \rightarrow Y$ and $g: X \rightarrow Y$ is a continuous function $h: [0, 1] \times X \rightarrow Y$ such that $h(0, \cdot) = f$ and $h(1, \cdot) = g$. Informally, any homotopy defines a continuous family of functions $h(t, \cdot)$ that morphs f into g ; an isotopy between graph drawings is a special type of homotopy. Spaces X and Y are *homotopy-equivalent* if there are continuous functions $f: X \rightarrow Y$ and $g: Y \rightarrow X$ such that the compositions $g \circ f$ and $f \circ g$ are respectively homotopic to the identity functions on X and Y . Space X is *contractible* if it is homotopy-equivalent to a single point.

Let Γ be a straight-line triangulation of a convex polygon P with k interior vertices. Let $X(\Gamma)$ denote the space of all planar straight-line triangulations of P that are equivalent to Γ . Any triangulation equivalent to Γ can be described by the locations of its interior vertices, so we can regard $X(\Gamma)$ as a subspace of \mathbb{R}^{2k} . Cairns’ morphing theorem [9, 10] implies that the space $X(\Gamma)$ is connected. Bloch, Connelly, and Henderson [7] proved that the space $X(\Gamma)$ is actually contractible. Simpler proofs of this theorem were recently given by Cerf [11] and Luo [47]. In particular, Luo observed that the Bloch–Connelly–Henderson theorem follows immediately from Floater’s barycentric embedding result; his argument applies more generally to strictly convex drawings of 3-connected planar graphs.

Steinitz’s classical proof of his polyhedral morphing theorem [57] implies a similar structural theorem for polyhedral representations of 3-connected planar graphs; see Richter-Gebert [54, Section 13.3].

Connelly, Henderson, Ho, and Starbird [18] conjectured that every isotopy class of geodesic triangulations on *any* surface S with constant curvature is homotopy-equivalent to the group $Isom_0(S)$ of isometries of S that are homotopic to the identity. In particular, $Isom_0(S^2)$ is the

rotation group $SO(3)$ and $Isom_0(\mathbb{T})$ is the translation group $S^1 \times S^1$; for every other orientable surface S without boundary, $Isom_0(S)$ is trivial [53]. Very recently, Luo, Wu, and Zhu proved this conjecture for all surfaces of genus at least 2 [48] and for the flat torus [49]; both proofs rely on nontrivial extensions of Floater’s theorem.

Here we offer a simpler proof for the flat-toroidal setting; in fact, we prove a more general result about convex drawings instead of just triangulations.

Theorem 6 *For any convex drawing Γ on the flat torus \mathbb{T} , the space of all convex drawings on \mathbb{T} that are isotopic to Γ is homotopy equivalent to \mathbb{T} .*

Proof: Fix a convex drawing Γ of a graph G with n vertices and m edges; without loss of generality, assume some vertex v is positioned at $(0, 0)$. Let $X = X(\Gamma)$ denote the space of all convex drawings of G isotopic to Γ , and let $X_0 = X_0(\Gamma)$ be the subspace of drawings in X where vertex v is positioned at $(0, 0)$. Every drawing in X is a translation of a unique drawing in X_0 , so $X = X_0 \times S^1 \times S^1$. Thus, to prove the theorem, it suffices to prove that X_0 is contractible.

Call a weight vector $\lambda \in \mathbb{R}_+^{2m}$ for Γ *normalized* if $\sum_d \lambda_d = 1$, where the sum is over all darts of Γ . Let $R = R(\Gamma)$ denote the set of all realizable weight vectors for T , and let $\overline{M} = \overline{M}(\Gamma)$ denote the set of all normalized morphable weight vectors for T .

Lemma 3 implies that \overline{M} is convex and therefore contractible. (Specifically, \overline{M} is the interior of a $(2m - n - 2)$ -dimensional convex polytope in \mathbb{R}^{2m} .)

Call two realizable weight vectors $\lambda, \lambda' \in R$ *equivalent* if there is a scaling vector $\alpha \in \mathbb{R}_+^n$ such that $\lambda'_d = \alpha_{tail(d)} \lambda_d$ for every dart d . Because the Laplacian matrix L^λ has rank $n - 1$, Lemma 6 implies that every realizable weight $\lambda \in R$ is equivalent to a *unique* normalized morphable weight $\mu \in \overline{M}$. It follows that R is homeomorphic to $\overline{M} \times \mathbb{R}_+^n$ and therefore contractible.

Now we follow the proof of Theorem 1.4 in Luo *et al.* [48]. Because every morphable weight is realizable, solving linear system (2) gives us a continuous map $\Phi: R \rightarrow X_0$. Floater’s mean-value weights [29, 40] give us a continuous map $\Psi: X_0 \rightarrow R$ such that $\Phi \circ \Psi$ is the identity map on X_0 . Because R is contractible, the function $\Psi \circ \Phi$ is homotopic to the identity map on R . We conclude that X_0 is homotopy equivalent to R and therefore contractible. \square

5 Open Questions

It is natural to ask whether our “best-of-both-worlds” planar morph can be extended to drawings on the flat torus. In Appendix B, we prove a toroidal analog of Lemma 1 for *realizable* weight vectors; unfortunately, the main roadblock is that not all weight vectors are realizable. In particular, given a realizable weight vector (morphable or not), it is not clear when changing the weights for a single edge results in another realizable weight vector.

Several previous planar morphing algorithms [1, 5, 19, 42] rely on a certain convexifying procedure [13, 38, 42, 43] and are (potentially) faster than our algorithm via the implementation recently described by Klemz [43]. It is an open question whether this convexification procedure can be extended to geodesic toroidal drawings.

One can also ask if the result can be extended to surfaces of higher genus. The recent results of Luo *et al.* [48] imply that Floater and Gotsman’s planar morphing algorithm [30] extends to geodesic triangulations on higher-genus surfaces of negative curvature; however, the existence of (any reasonable analog of) piecewise-linear morphs on such surfaces remains unknown.

Acknowledgments

We thank Anna Lubiw for asking questions about Lemma 5.1 of Chambers *et al.* [12], whose answers ultimately led to the discovery of Theorem 3, and for other helpful feedback. We also thank Yanwen Luo for making us aware of his recent work [47–49]. Finally, we thank the anonymous reviewers of both the conference version [26] and journal version of this paper for their comments and helpful suggestions for improvement.

References

- [1] S. Alamdari, P. Angelini, F. Barrera-Cruz, T. M. Chan, G. Da Lozzo, G. Di Battista, F. Frati, P. Haxell, A. Lubiw, M. Patrignani, V. Roselli, S. Singla, and B. T. Wilkinson. How to morph planar graph drawings. *SIAM J. Comput.*, 46(2):824–852, 2017. doi:10.1137/16M1069171.
- [2] L. Aleksandrov and H. Djidjev. Linear algorithms for partitioning embedded graphs of bounded genus. *SIAM J. Discrete Math.*, 9(1):129–150, 1996. doi:10.1137/S0895480194272183.
- [3] J. Alman and V. Vassilevska Williams. A refined laser method and faster matrix multiplication. In *Proc. 32nd Ann. ACM-SIAM Symp. Discrete Algorithms*, October 2021. doi:0.1137/1.9781611976465.32.
- [4] N. Alon and R. Yuster. Matrix sparsification and nested dissection over arbitrary fields. *J. ACM*, 60(4):25:1–25:8, 2013. doi:10.1145/2508028.2505989.
- [5] P. Angelini, G. Da Lozzo, F. Frati, A. Lubiw, M. Patrignani, and V. Roselli. Optimal morphs of convex drawings. In *Proc. 31st Int. Symp. Comput. Geom.*, number 34 in Leibniz Int. Proc. Informatics, pages 126–140, 2015. doi:10.4230/LIPIcs.SOCG.2015.126.
- [6] E. H. Bareiss. Sylvester’s identity and multistep integer-preserving Gaussian elimination. *Math. Comput.*, 22(103):565–578, 1968. doi:10.2307/2004533.
- [7] E. D. Bloch, R. Connelly, and D. W. Henderson. The space of simplexwise linear homeomorphisms of a convex 2-disk. *Topology*, 23(2):161–175, 1984. doi:10.1016/0040-9383(84)90037-5.
- [8] C. W. Borchardt. Ueber eine der interpolation entsprechende Darstellung der Eliminations-Resultante. *J. Reine Angew. Math.*, 57:111–121, 1860. doi:10.1515/crll.1860.57.111.
- [9] S. S. Cairns. Deformations of plane rectilinear complexes. *Amer. Math. Monthly*, 51(5):247–252, 1944. doi:10.2307/2304300.
- [10] S. S. Cairns. Isotopic deformations of geodesic complexes on the 2-sphere and on the plane. *Ann. Math.*, 45(2):207–217, 1944. doi:10.2307/1969263.
- [11] J. Cerf. About the Bloch–Connelly–Henderson theorem on the simplexwise linear homeomorphisms of a convex 2-disk. Preprint, October 2019. doi:10.48550/arXiv.1910.00240.
- [12] E. W. Chambers, J. Erickson, P. Lin, and S. Parsa. How to morph graphs on the torus. In *Proc. 32nd Ann. ACM-SIAM Symp. Discrete Algorithms*, pages 2759–2778, 2021. doi:10.1137/1.9781611976465.164.

- [13] M. Chrobak, M. T. Goodrich, and R. Tamassia. Convex drawings of graphs in two and three dimensions (preliminary version). In *Proc. 12th Ann. Symp. Comput. Geom.*, pages 319–328, 1996. doi:10.1145/237218.237401.
- [14] M. B. Cohen, J. Kelner, J. Peebles, R. Peng, A. Sidford, and A. Vladu. Faster algorithms for computing the stationary distribution, simulating random walks, and more. In *Proc. 57th Ann. IEEE Symp. Found. Comput. Sci.*, pages 583–592, 2016. doi:10.1109/FOCS.2016.69.
- [15] É. Colin de Verdière and A. de Mesmay. Testing graph isotopy on surfaces. *Discrete Comput. Geom.*, 51(1):171–206, 2014. doi:10.1007/s00454-013-9555-4.
- [16] É. Colin de Verdière, M. Pocchiola, and G. Vegter. Tutte’s barycenter method applied to isotopies. *Comput. Geom. Theory Appl.*, 26(1):81–97, 2003. doi:10.1016/S0925-7721(02)00174-8.
- [17] Y. Colin de Verdière. Comment rendre géodésique une triangulation d’une surface? *L’Enseignement Mathématique*, 37:201–212, 1991. doi:10.5169/seals-58738.
- [18] R. Connelly, D. W. Henderson, C. W. Ho, and M. Starbird. On the problems related to linear homeomorphisms, embeddings, and isotopies. In *Continua, Decompositions, Manifolds: Proc. Texas Topology Symposium, 1980*, pages 229–239. Univ. Texas Press, 1983.
- [19] G. Da Lozzo, G. Di Battista, F. Frati, M. Patrignani, and V. Roselli. Upward planar morphs. *Algorithmica*, 82(10):2985–3017, 2020. doi:10.1007/s00453-020-00714-6.
- [20] P. De Leenheer. An elementary proof of a matrix tree theorem for directed graphs. *SIAM Review*, 62(3):716–726, 2020. doi:10.1137/19M1265193.
- [21] O. Delgado-Friedrichs. Barycentric drawings of periodic graphs. In *Proc. 11th Symp. Graph Drawing*, number 2912 in Lecture Notes Comput. Sci., pages 178–189, 2003. doi:10.1007/978-3-540-24595-7_17.
- [22] O. Delgado-Friedrichs. Equilibrium placement of periodic graphs and convexity of plane tilings. *Discrete Comput. Geom.*, 33(1):67–81, 2004. doi:10.1007/s00454-004-1147-x.
- [23] G. Di Battista and F. Frati. From Tutte to Floater and Gotsman: On the resolution of planar straight-line drawings and morphs. In H. C. Purchase and I. Rutter, editors, *Proc. 29th Int. Symp. Graph Drawing Network Vis.*, number 12868 in Lecture Notes Comput. Sci., pages 109–122. Springer, 2021. doi:10.1007/978-3-030-92931-2_8.
- [24] P. Eades and P. Garvan. Drawing stressed planar graphs in three dimensions. In *Proc. 2nd Symp. Graph Drawing*, number 1027 in Lecture Notes Comput. Sci., pages 212–223, 1995. doi:10.1007/BFb0021805.
- [25] J. Erickson and P. Lin. A toroidal Maxwell-Cremona-Delaunay correspondence. In *Proc. 36th Int. Symp. Comput. Geom.*, number 164 in Leibniz Int. Proc. Informatics, pages 40:1–40:17. Schloss Dagstuhl–Leibniz-Zentrum für Informatik, 2020. doi:10.4230/LIPIcs.SoCG.2020.40.
- [26] J. Erickson and P. Lin. Planar and toroidal morphs made easier. In *Proc. 29th Int. Symp. Graph Drawing Network Vis.*, number 12868 in Lecture Notes Comput. Sci., pages 123–137, 2021. doi:10.1007/978-3-030-92931-2_9.

- [27] M. S. Floater. Parametrization and smooth approximation of surface triangulations. *Comp. Aided Geom. Design*, 14(3):231–250, 1997. doi:10.1016/S0167-8396(96)00031-3.
- [28] M. S. Floater. Parametric tilings and scattered data approximation. *Int. J. Shape Modeling*, 4(3–4):165–182, 1998. doi:10.1142/S021865439800012X.
- [29] M. S. Floater. Mean value coordinates. *Comput. Aided Geom. Design*, 20(1):19–27, 2003. doi:10.1016/S0167-8396(03)00002-5.
- [30] M. S. Floater and C. Gotsman. How to morph tilings injectively. *J. Comput. Appl. Math.*, 101(1–2):117–129, 1999. doi:10.1016/S0377-0427(98)00202-7.
- [31] S. J. Gortler, C. Gotsman, and D. Thurston. Discrete one-forms on meshes and applications to 3D mesh parameterization. *Comput. Aided Geom. Design*, 23(2):83–112, 2006. doi:10.1016/j.cagd.2005.05.002.
- [32] C. Gotsman and V. Surazhsky. Guaranteed intersection-free polygon morphing. *Computers & Graphics*, 25(1):67–75, 2001. doi:10.1016/S0097-8493(00)00108-4.
- [33] D. H. Greene. The decomposition of polygons into convex parts. In F. P. Preparata, editor, *Computational Geometry*, volume 1 of *Advances in Computing Research*. JAI Press, 1983.
- [34] R. Haas, D. Orden, G. Rote, F. Santos, B. Servatius, H. Servatius, D. Souvaine, I. Streinu, and W. Whiteley. Planar minimally rigid graphs and pseudo-triangulations. *Comput. Geom. Theory Appl.*, 31(1–2):31–61, 2005. doi:10.1016/j.comgeo.2004.07.003.
- [35] J. Hass and P. Scott. Simplicial energy and simplicial harmonic maps. *Asian J. Math.*, 19(4):593–636, 2015. doi:10.4310/AJM.2015.v19.n4.a2.
- [36] A. Hatcher. *Algebraic Topology*. Cambridge Univ. Press, 2002. URL: <http://www.math.cornell.edu/~hatcher/AT/ATpage.html>.
- [37] S. Hertel and K. Mehlhorn. Fast triangulation of the plane with respect to simple polygons. *Inf. Control*, 64(1–3):52–76, 1985. doi:10.1016/S0019-9958(85)80044-9.
- [38] S.-H. Hong and H. Nagamochi. Convex drawings of hierarchical planar graphs and clustered planar graphs. *J. Discrete Algorithms*, 8(3):282–295, 2010. doi:10.1016/j.jda.2009.05.003.
- [39] J. E. Hopcroft and P. J. Kahn. A paradigm for robust geometric algorithms. *Algorithmica*, 7(1–6):339–380, 1992. doi:10.1007/BF01758769.
- [40] K. Hormann and M. S. Floater. Mean value coordinates for arbitrary planar polygons. *ACM Trans. Graphics*, 25(4):1424–1441, 2006. doi:10.1145/1183287.1183295.
- [41] M. Keil and J. Snoeyink. On the time bound for convex decomposition of simple polygons. *Int. J. Comput. Geom. Appl.*, 12(3):181–192, 2002. doi:10.1142/S0218195902000803.
- [42] L. Kleist, B. Klemz, A. Lubiw, L. Schlipf, F. Staals, and D. Strash. Convexity-increasing morphs of planar graphs. *Comput. Geom. Theory Appl.*, 84:69–88, 2019. doi:10.1016/j.comgeo.2019.07.007.

- [43] B. Klemz. Convex drawings of hierarchical graphs in linear time, with applications to planar graph morphing. In *Proc. 29th Ann. Europ. Symp. Algorithms*, number 204 in Leibniz Int. Proc. Informatics, pages 57:1–57:15, 2021. doi:10.4230/LIPIcs.ESA.2021.68.
- [44] F. Le Gall. Powers of tensors and fast matrix multiplication. In *Proc. 25th int. Symb. Alg. Comput.*, pages 296–303, 2014. doi:10.1145/2608628.2608664.
- [45] R. J. Lipton, D. J. Rose, and R. E. Tarjan. Generalized nested dissection. *SIAM J. Numer. Anal.*, 16:346–358, 1979. doi:10.1137/0716027.
- [46] L. Lovász. Discrete analytic functions: An exposition. In A. Grigor’yan and S.-T. Yau, editors, *Eigenvalues of Laplacians and other geometric operators*, number 9 in Surveys in Differential Geometry, pages 241–273. Int. Press, 2004. doi:10.4310/SDG.2004.v9.n1.a7.
- [47] Y. Luo. Spaces of geodesic triangulations of surfaces. *Discrete Comput. Geom.*, 68(3):709–727, 2022. doi:10.1007/s00454-021-00359-4.
- [48] Y. Luo, T. Wu, and X. Zhu. The deformation space of geodesic triangulations and generalized Tutte’s embedding theorem. Preprint, May 2021. doi:10.48550/arXiv.2105.00612.
- [49] Y. Luo, T. Wu, and X. Zhu. The deformation space of geodesic triangulations of flat tori. Preprint, July 2021. doi:10.48550/arXiv.2107.05159.
- [50] B. Mohar. Circle packings of maps—The Euclidean case. *Rend. Sem. Mat. Fis. Milano*, 67(1):191–206, 1997. doi:10.1007/BF02930499.
- [51] B. Mohar. Circle packings of maps in polynomial time. *Europ. J. Combin.*, 18(7):785–805, 1997. doi:10.1006/eujc.1996.0135.
- [52] J. R. Munkres. *Topology*. Prentice-Hall, 2nd edition, 2000.
- [53] D. A. Norris. Isometries homotopic to the identity. *Proc. Amer. Math. Soc.*, 105(3):692–696, 1989. doi:10.2307/2046921.
- [54] J. Richter-Gebert. *Realization spaces of polytopes*. Number 1643 in Lecture Notes Math. Springer, 1996. doi:10.1007/BFb0093761.
- [55] H. Shen, Z. Jiang, D. Zorin, and D. Panozzo. Progressive embedding. *ACM Trans. Graphics*, 38(4):32:1–32:13, 2019. Proc. SIGGRAPH 2019. doi:10.1145/3306346.3323012.
- [56] D. Steiner and A. Fischer. Planar parameterization for closed 2-manifold genus-1 meshes. In *Proc. 9th ACM Symp. Solid Modeling Appl.*, pages 83–91, 2004. doi:10.2312/sm.20041379.
- [57] E. Steinitz and H. Rademacher. *Vorlesungen über die Theorie der Polyeder: unter Einschluß der Elemente der Topologie*. Number 41 in Grundlehren der mathematischen Wissenschaften. Springer-Verlag, 1934. Reprinted 1976.
- [58] V. Surazhsky and C. Gotsman. Controllable morphing of compatible planar triangulations. *ACM Trans. Graphics*, 20(4):203–231, 2001. doi:10.1145/502783.502784.
- [59] V. Surazhsky and C. Gotsman. Morphing stick figures using optimal compatible triangulations. In *Proc. 9th Pacific Conf. Comput. Graphics Appl.*, pages 40–49, 2001. doi:10.1109/PCCGA.2001.962856.

- [60] V. Surazhsky and C. Gotsman. Intrinsic morphing of compatible triangulations. *Int. J. Shape Modeling*, 9(2):191–201, 2003. doi:10.1142/S0218654303000115.
- [61] C. Thomassen. Deformations of plane graphs. *J. Comb. Theory Ser. B*, 34(3):244–257, 1983. doi:10.1016/0095-8956(83)90038-2.
- [62] C. Thomassen. Tutte’s spring theorem. *J. Graph Theory*, 45(4):275–280, 2004. doi:10.1002/jgt.10163.
- [63] W. T. Tutte. The dissection of equilateral triangles into equilateral triangles. *Math. Proc. Cambridge Phil. Soc.*, 44(4):463–482, 1948. doi:10.1017/S030500410002449X.
- [64] W. T. Tutte. How to draw a graph. *Proc. London Math. Soc.*, 13(3):743–768, 1963. doi:10.1112/plms/s3-13.1.743.

A Some Bad Examples

Here we provide several concrete examples showing that barycentric methods for drawing and morphing planar graphs do not immediately generalize to drawings on the flat torus.

First, we give an infinite family of non-realizable positive weight vectors. Let G be *any* toroidal graph, and consider the weight vector λ that assigns weight 2 to a single dart d and weight 1 to every dart other than d . (There is nothing special about the values 1 and 2 here: one can replace 1 and 2 with any two distinct integers and obtain a similar result.)

Lemma 7 λ is not a realizable weight vector for G .

Proof: Let $u = \text{tail}(d)$ and $v = \text{head}(d)$. For the sake of argument, suppose the linear system $L^\lambda P = H^\lambda$ has a solution; let Γ^λ be the resulting drawing. This system remains solvable if we remove row u and arbitrarily fix p_u [56]. All dart weights in this truncated linear system are equal to 1, which implies that the drawing Γ^λ is identical to the Floater drawing Γ^1 for the all-1s weight vector. Comparing the two linear systems, we conclude that $p_v - p_u + \tau_d = (0, 0)$; that is, the edge of d has length zero in $\Gamma^\lambda = \Gamma^1$. But this is impossible; every edge in a Tutte drawing has non-zero length [31, Lemma B.5]. \square

Next, we give an example of two realizable weight vectors for the same torus graph whose averages are not realizable. Consider the toroidal drawings of K_7 shown in Figure 7, which differ only in the position of vertex 2. We computed mean-value weights λ and μ for these drawings, normalized so that the weights of all edges leaving each vertex sum to 1 [29, 40]. Routine calculations (which we implemented in Python) now imply that the average weight $(\lambda + \mu)/2$ is not realizable.

Finally, we consider Steiner and Fischer’s approach [56] of fixing a single vertex, which restores the Laplacian linear system to full rank. The top row of Figure 8 shows two isotopic drawings of a 12×12 toroidal grid, one with a single row of vertices shifted $1/2$ to the left, the other with a single column of vertices shifted $1/2$ downward. Let λ^\leftarrow and λ^\downarrow respectively denote the normalized mean-value weights for these drawings [29, 40]. The bottom left image in Figure 8 shows the Steiner-Fischer drawing for the weight $\lambda = (2\lambda^\leftarrow + \lambda^\downarrow)/3$, with the red edges indicating the fixed vertex. This drawing is clearly not crossing-free; it also follows that the weight vector λ is not realizable.

The bottom right of Figure 8 shows the corresponding Floater drawing for the realizable weight vector $\mu = (2\mu^\leftarrow + \mu^\downarrow)/3$, where μ^\leftarrow and μ^\downarrow are *morphable* weights derived by rescaling λ^\leftarrow and λ^\downarrow , as described in Lemma 6.

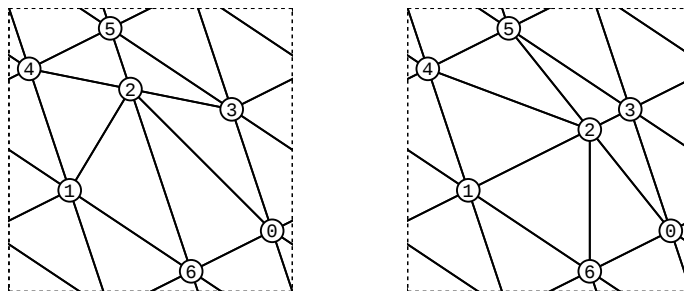


Figure 7: Isotopic drawings of K_7 whose normalized mean-value weights are not morphable.

Steiner and Fischer claim [56, Section 2.2.1] that their drawings have no “foldovers” except possibly at the fixed vertex and its neighbors. Here a “foldover” occurs at a vertex of a drawing if the faces incident to that vertex overlap in the drawing (where formally, faces are determined by the reference drawing used to define the translation vectors). Close examination of the bottom left image of Figure 8 shows that this claim is incorrect: there are “foldovers” at several vertices that are neither the fixed vertex nor its neighbors.

B Trying to Morph Toroidal Drawings Edge by Edge

Colin de Verdière [17] showed that all *symmetric* positive weights are realizable on the flat torus (see also [22, 31, 35, 46]); Chambers *et al.* [12] exploit this observation in their morphing algorithm.

The following lemma generalizes Lemma 1 to the toroidal setting; it also generalizes Lemma 5.1 of Chambers *et al.* [12] to work for *asymmetric* weights; however, it is unclear in the asymmetric case when changing the weights for a single edge in a realizable weight vector results in another realizable weight vector.

Lemma 8 *Let λ and μ be arbitrary realizable weight vectors such that $\lambda_d \neq \mu_d$ or $\lambda_{\text{rev}(d)} \neq \mu_{\text{rev}(d)}$ for some dart d , and $\lambda_{d'} = \mu_{d'}$ for all darts $d' \notin \{d, \text{rev}(d)\}$. For every vertex w , the vector $p_w^\mu - p_w^\lambda$ is parallel to the drawing of d in Γ^λ .*

Proof: Suppose d has tail u and head v . By the definition of crossing vectors, dart d appears in Γ^λ as the projection of a dart in the universal cover from p_u^λ to $p_v^\lambda + \tau_d$. Fix a non-zero vector $\sigma \in \mathbb{R}^2$ orthogonal to the vector $p_v^\lambda - p_u^\lambda + \tau_d$ and thus orthogonal to darts $\{d, \text{rev}(d)\}$ in Γ^λ . For each vertex i , let $z_i^\lambda = p_i^\lambda \cdot \sigma$ and $z_i^\mu = p_i^\mu \cdot \sigma$, and for each dart d' , let $\chi_{d'} = \tau_{d'} \cdot \sigma$. Our choice of σ implies that $\chi_d = z_u^\lambda - z_v^\lambda$. We need to prove that $z_i^\lambda = z_i^\mu$ for every vertex i .

Let $X^\lambda = H^\lambda \cdot \sigma$ and $X^\mu = H^\mu \cdot \sigma$. The real vector $Z^\lambda = (z_i^\lambda)_i$ is a solution to the linear system $L^\lambda Z = X^\lambda$; in fact, Z^λ is the *unique* solution such that $z_n^\lambda = 0$. Similarly, $Z^\mu = (z_i^\mu)_i$ is the unique solution to an analogous equation $L^\mu Z = X^\mu$ with $z_n^\mu = 0$. We will prove that $L^\mu Z^\lambda = X^\mu$, so that in fact $Z^\lambda = Z^\mu$.

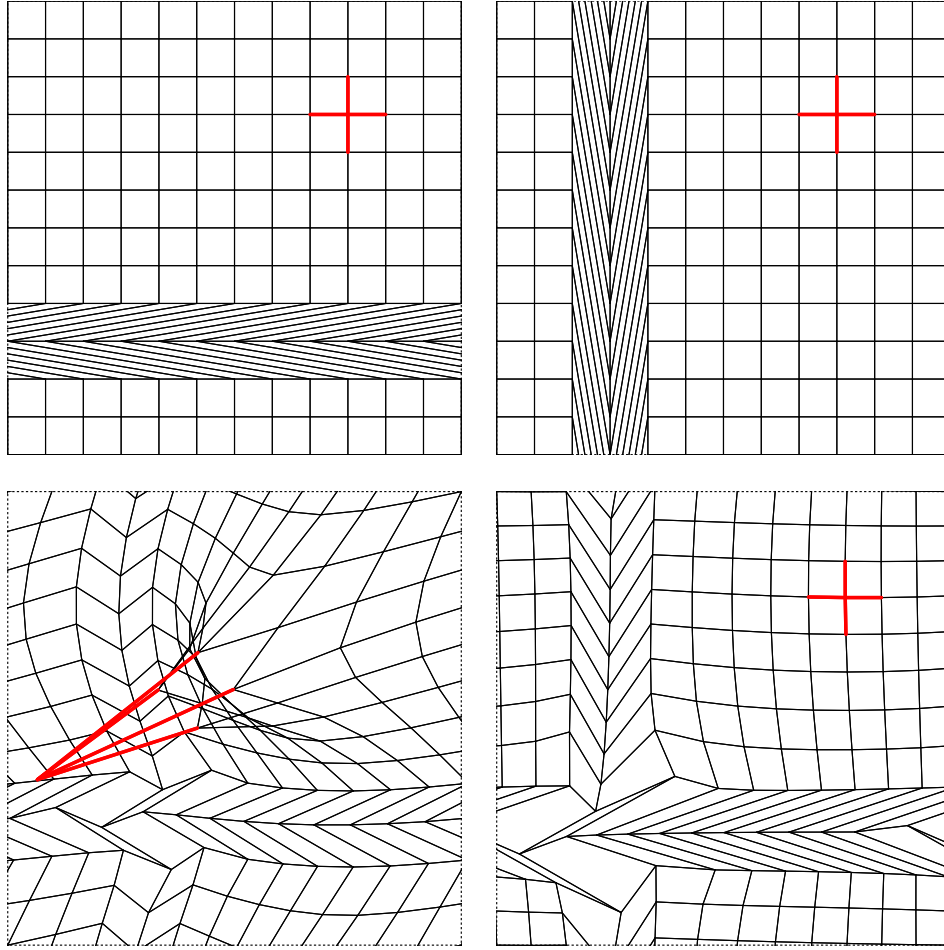


Figure 8: A bad example of fixed-vertex weight interpolation; see the text for explanation.

Let $\delta = \mu_d - \lambda_d$ and $\varepsilon = \mu_{rev(d)} - \lambda_{rev(d)}$. The matrices L^λ and L^μ differ in only four locations:

$$L_{ij}^\mu - L_{ij}^\lambda = \begin{cases} \delta & \text{if } (i, j) = (u, u) \\ -\delta & \text{if } (i, j) = (u, v) \\ -\varepsilon & \text{if } (i, j) = (v, u) \\ \varepsilon & \text{if } (i, j) = (v, v) \\ 0 & \text{otherwise} \end{cases}$$

More concisely, we have $L^\mu = L^\lambda + (\delta \mathbf{e}_u - \varepsilon \mathbf{e}_v)(\mathbf{e}_u - \mathbf{e}_v)^T$. Similar calculations imply $H^\mu = H^\lambda + \tau_d(\delta \mathbf{e}_u - \varepsilon \mathbf{e}_v)$ and therefore $X^\mu = X^\lambda + \chi_d(\delta \mathbf{e}_u - \varepsilon \mathbf{e}_v)$. It follows that

$$\begin{aligned} L^\mu Z^\lambda &= L^\lambda Z^\lambda + (\delta \mathbf{e}_u - \varepsilon \mathbf{e}_v)(\mathbf{e}_u - \mathbf{e}_v)^T Z^\lambda \\ &= X^\lambda + (\delta \mathbf{e}_u - \varepsilon \mathbf{e}_v)(z_u^\lambda - z_v^\lambda) \end{aligned}$$

$$\begin{aligned}
&= X^\lambda + (\delta \mathbf{e}_u - \varepsilon \mathbf{e}_v) \chi_d \\
&= X^\mu,
\end{aligned}$$

completing the proof. \square

We obtain the following partial result towards understanding when changing weights for a single edge in a realizable weight vector results in another realizable weight vector, via the analyses of Lemmas 6 and 8.

Lemma 9 *Let λ be a realizable weight vector, and let α be a positive row vector such that $\alpha L^\lambda = (0, \dots, 0)$ and $\alpha H^\lambda = (0, 0)$. Let μ be another positive weight vector such that $\lambda_d \neq \mu_d$ or $\lambda_{\text{rev}(d)} \neq \mu_{\text{rev}(d)}$ for some dart d , and $\lambda_{d'} = \mu_{d'}$ for all darts $d' \notin \{d, \text{rev}(d)\}$. Set $\delta := \mu_d - \lambda_d$ and $\varepsilon := \mu_{\text{rev}(d)} - \lambda_{\text{rev}(d)}$. If $\delta \alpha_{\text{tail}(d)} = \varepsilon \alpha_{\text{head}(d)}$, then μ is realizable.*

Proof: Suppose d has tail u and head v . The analysis of Lemma 8 gives us

$$\begin{aligned}
L^\mu &= L^\lambda + (\delta \mathbf{e}_u - \varepsilon \mathbf{e}_v) (\mathbf{e}_u - \mathbf{e}_v)^T \\
H^\mu &= H^\lambda + \tau_d (\delta \mathbf{e}_u - \varepsilon \mathbf{e}_v)
\end{aligned}$$

Because $\alpha L^\lambda = (0, \dots, 0)$ and $\alpha H^\lambda = (0, 0)$, we immediately have $\alpha L^\mu = (\delta \alpha_u - \varepsilon \alpha_v) (\mathbf{e}_u - \mathbf{e}_v)^T$ and $\alpha H^\mu = x_d (\delta \alpha_u - \varepsilon \alpha_v)$.

If $\delta \alpha_u = \varepsilon \alpha_v$, then $\alpha L^\mu = (0, \dots, 0)$ and $\alpha H^\mu = (0, 0)$. It follows that a suitable scaling of μ is morphable, and therefore realizable, which implies that μ itself is also realizable. \square

In particular, when λ is symmetric, then we can choose α to be the all-1s vector, which implies that any weight μ satisfying the conditions of Lemma 9 is also symmetric.